

# Optimal Wrist Design of Wrist-hollow Type 6-axis Articulated Robot using Genetic Algorithm

Hyeon Min Jo\*, Won Jee Chung\*<sup>#</sup>, Seung Min Bae\*, Jong Kap Choi\*, Dae Young Kim\*,  
Yeon Joo Ahn\*\*, Hee Sung Ahn\*\*\*

\*Mechanical Design, Changwon national UNIV., \*\*Robot Valley, \*\*\*OTO Robotics

## 유전자 알고리즘을 이용한 손목 중공형 6축 수직다관절 로봇의 최적 손목 설계에 관한 연구

조현민\*, 정원지\*<sup>#</sup>, 배승민\*, 최종갑\*, 김대영\*, 안연주\*\*, 안희성\*\*\*

\*국립 창원대학교 기계설계공학과, \*\*(주)로봇밸리, \*\*(주)오토로보틱스

(Received 20 July 2018; received in revised form 26 July 2018; accepted 30 July 2018)

### ABSTRACT

In arc-welding applying to the present automobile part manufacturing process, a wrist-hollow type arc welding robot can shorten the welding cycle time, because feedability of a welding wire is not affected by a robot posture and thus facilitates high-quality arc welding, based on stable feeding with no entanglement. In this paper, we will propose the optimization of wrist design for a wrist-hollow type 6-Axis articulated robot. Specifically, we will perform the investigation on the optimized design of inner diameter of hollow arms (Axis 4 and Axis 6) and width of the upper arm by using the simulation of robot motion characteristics, using a Genetic Algorithm (i.e., GA). Our simulations are based on SolidWorks<sup>®</sup> for robot modeling, MATLAB<sup>®</sup> for GA optimization, and RecurDyn<sup>®</sup> for analyzing dynamic characteristics of a robot. Especially RecurDyn<sup>®</sup> is incorporated in the GA module of MATLAB<sup>®</sup> for the optimization process. The results of the simulations will be verified by using RecurDyn<sup>®</sup> to show that the driving torque of each axis of the wrist-hollow 6-axis robot with the optimized wrist design should be smaller than the rated output torque of each joint servomotor. Our paper will be a guide for improving the wrist-hollow design by optimizing the wrist shape at a detail design stage when the driving torque of each joint for the wrist-hollow 6-axis robot (to be developed) is not matched with the servomotor specifications.

**Key Words :** Wrist-hollow Type(중공형), Arc Welding(아크 용접), 6-axis Articulated Robot(6축 수직다관절 로봇), Genetic Algorithm(유전자 알고리즘), RecurDyn<sup>®</sup>

### 1. Introduction

Due to the shortening cycle of new vehicle

model development, the application of offline programming (OLP) to welding robot systems is indispensable in arc welding for automotive part manufacturing processes. However, the interference of cables limits the range of motion of robot

# Corresponding Author : [wjchung@changwon.ac.kr](mailto:wjchung@changwon.ac.kr)

Tel: +82-55-267-1138, Fax: +82-55-263-5221

systems in which conventional welding cables are installed as the external type. Therefore, after the robots are deployed in the plant, the downloaded robot programs need to be modified in OLP, which is cumbersome. Recently, to overcome this shortcoming, hollow robots with embedded welding cable have been developed and are becoming the main products in the welding robot market.<sup>[1]</sup>

Conventional universal welding robots have the problems of difficulty in welding the front side of the robot and unstable welding quality due to the interference of the torch cable and torch clamp with the robot arms and the bending of torch cables. However, arc welding-specialized robots of the hollow wrist type are not affected by robot posture for the feedability of welding wires. Thus, they can shorten the welding cycle time and achieve high-quality arc-welding through stable feeding that prevents twists.

Subjects of high interest with respect to the industrial manipulators of industrial robots are the control system, orbit planning, machine design, and computer vision. Tasks by the manipulator include motions caused by the force/torque applied by single or multiple actuators. The main purpose of control is to set the positions and directions of the wrist and tools with the desired precision and speed considering the reaction force, inertia force, and gravity load of the link.<sup>[2]</sup>

The trajectory accuracy of the weld line is extremely important because advanced technologies, such as weaving, are required for recent welding robots. It is greatly dependent on the torque characteristics according to the control system and robot arm shape and directly affects the welding quality. To overcome this shortcoming, the design of the robot arm in accordance with the torque characteristics is essential. This will improve the efficiency and precision of the six-axis articulated robot and make a significant contribution to the welding robot industry by achieving a remarkable

improvement in the operation of robots.<sup>[1]</sup>

Almost every paper in this field until now has addressed the optimization of the control system and sensor arrangement.<sup>[2,3]</sup> Jeon<sup>[5]</sup> compares the dynamic characteristics of the motor and reducer selected in the basic design stage of wrist-solid type four-axis robots with the dynamic characteristics required for actual operation. However, he does not explain the methods to complete the design when the specifications are inadequate.

This study suggests a method of improving the design by performing optimization design using the genetic algorithm (GA) for the shape of the upper arm, such as the inner diameter of the hollow arm and the width of the upper arm when the specifications of the initial servo motor are inadequate and through the simulation of the dynamic characteristics of the robot.

## **2. Optimal Wrist Design of Hollow Six-axis Articulated Robot**

### **2.1 Conceptual design of six-axis articulated robot**

A six-axis hollow robot was designed in the concept development stage to develop a welding-specialized robot instead of a universal six-axis robot, and the structure is shown in Fig. 1. In a six-axis robot, axes 1, 2, 3, and 5 play the rotating role as well as the role of supporting the robot, and axes 4 and 6 are hollow types to embed the motor and welding cables. The weight of hollow motors increases exponentially with the increasing inner diameter. However, the inner diameter of the hollow hall must be at least 50 mm considering the thickness of welding and motor cables and thus set as a conditional function for GA optimization. The payload of the robot is 60N.

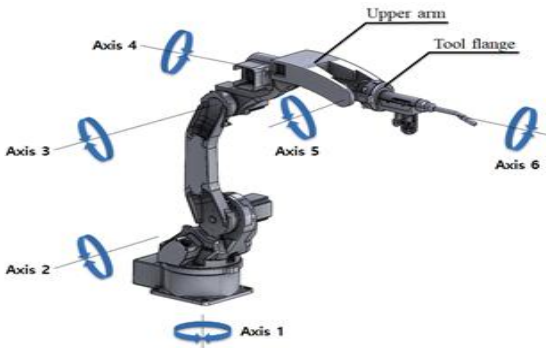


Fig. 1 The configuration of the 6-axis robot

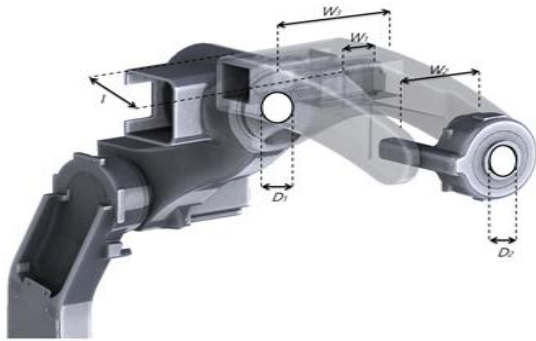


Fig. 2 Design variables to be optimized

Table 1 Dynamic analysis parameter of six-axis robot

| Axis  | 1    | 2   | 3   | 4    | 5    | 6    |
|---|------|-----|-----|------|------|------|
| Moment of inertia ( $\times 10^4 \text{ kg}\cdot\text{m}^2$ ) | 2.1  | 4.0 | 2.1 | 0.05 | 0.06 | 0.04 |
| Reduction gear ratio (:1)                                     | 164  | 164 | 149 | 81   | 87   | 50   |
| Transmission efficiency of Reducer                            | 0.8  |     |     |      |      |      |
| Maximum rotational speed of Motor (rpm)                       | 3000 |     |     |      |      |      |
| Acceleration and deceleration of the time (sec)               | 0.2  |     |     |      |      |      |

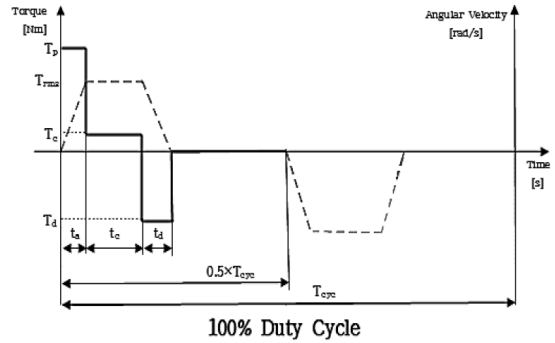


Fig. 3 Typical torque curve of an arm<sup>[5]</sup>

## 2.2 Optimization simulation

The design parameters to be optimized are  $D_1, D_2, W_1, W_2, W_3, l$ , which correspond to the upper arm, wrist, and tool flange of the robot, as shown in Fig. 2.

For the dynamic analysis of the robot, this study used RecurDyn<sup>®</sup>. In the first step of analysis, the reference speed profile of every axis should be created by considering the working cycle of the robot. For the parameters of each axis used as the inputs of RecurDyn<sup>®</sup>, the rotor inertia moment, reduction ratio, maximum rotation speed of the motor, and acceleration and deceleration time of the motor were considered, which are listed in Table 1. The structural shape of the arm was optimized by applying the above parameters using the GA optimization in MATLAB<sup>®</sup>. Considering the payload, the optimized robot arm must have sufficient torque for driving. In other words, the conditional function was set so that the maximum drive torque of each axis according to the robot arm shape would be less than the rated output torque of the used reducer and servo motor. This will be explained in more detail in Fig. 3.

The algorithm used in GA is shown in a block diagram in Fig. 4.

Here, elitecount is the number of objects that have the most adequate fitness value in the current generation that must be left to the next generation.

The default value of elitecount is 2. If the elitecount value is high, the search efficiency drops. For this reason, the elitecount value was set to 100, which is 2% of the population size of the generation. Furthermore,  $T_p$  is the maximum drive torque of each axis, and  $T_{rated}$  is the rated output torque of the servo motor of each joint. The stop condition of Fig. 3 requires that  $T_p$  is smaller than  $T_{rated}$ . To improve the accuracy of dynamic analysis, the friction effect between joints that come into contact with each other should be considered. In this study, a constant ( $\beta$ ), a ratio between a certain torque ( $T_a$ ) and an acceleration torque ( $T_b$ ) at a certain velocity, was introduced as an empirical value. Thus, the static friction coefficient of 0.5 and the dynamic friction coefficient of 0.3 were applied to RecurDyn®.

As shown in Fig. 4, as a result of applying these friction coefficients, the torque at constant speed  $T_c$  had non-zero values in pure horizontal motions.

The equation to obtain the torque pattern is as follows:[5]

$$\beta = \frac{T_c}{T_a} \quad (1)$$

$$T_a = \frac{J_L \times a_m}{\eta} + T_g \quad (2)$$

$$T_p = T_a + T_c \quad (3)$$

$$T_c = \beta + T_l \quad (4)$$

where  $J_L$  is the equivalent inertia moment of each motor,  $a_m$  is the angular acceleration of the motor,  $T_g$  is the torque generated by gravity, and  $T_p$  is the maximum torque required in the motor.[5]

### 3. Simulation Results

The reference speed profile appropriate for every axis was found by analyzing the motions of the six-axis robot during the working cycle, as shown in Fig. 5. A half-cycle was used for axis 1 because it was not affected by gravity as it moved horizontally. For other axes, a full cycle was used because they moved vertically and was affected by gravity. The reference speed profiles of all axes are summarized in Table 2, which were used to calculate the drive torque in Fig. 3.

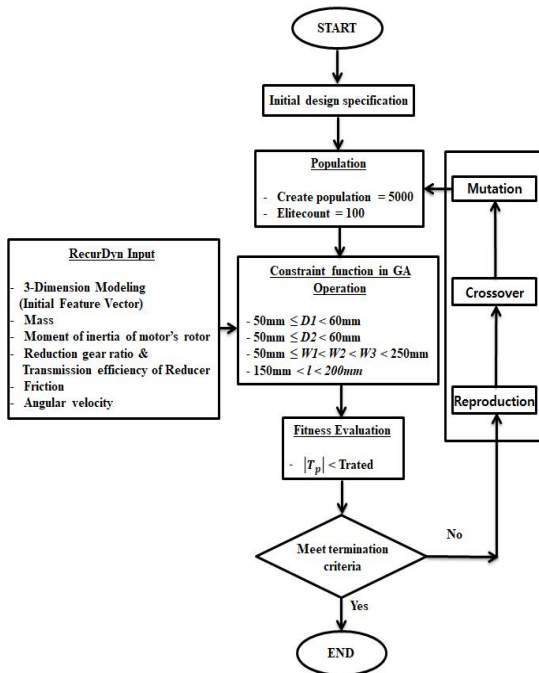
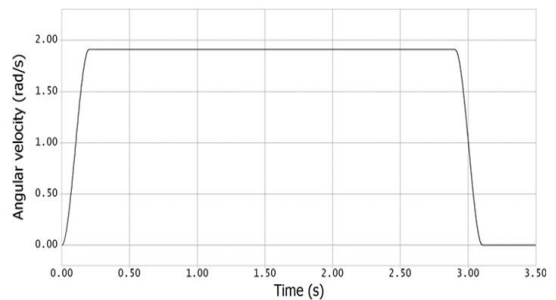
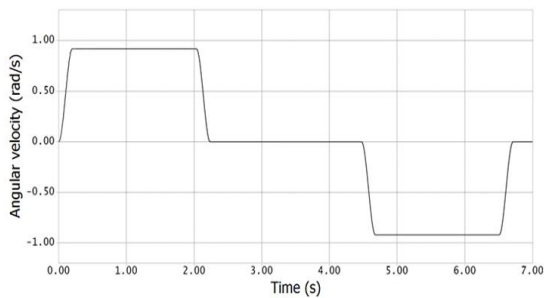


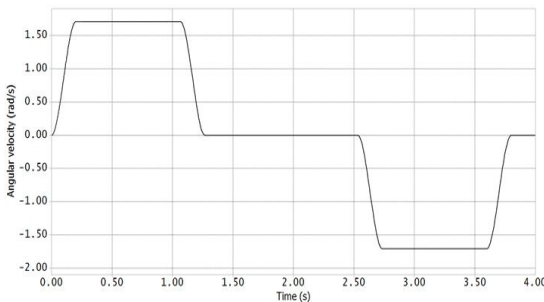
Fig. 4 Block diagram of GA simulation incorporating RecurDyn®



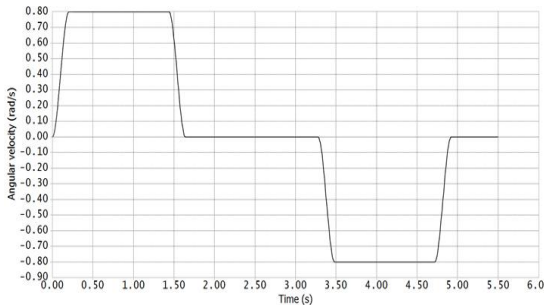
Axis 1



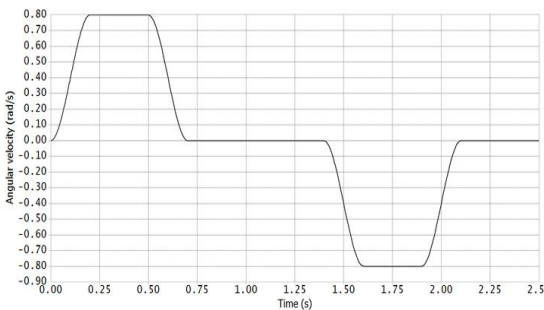
Axis 2



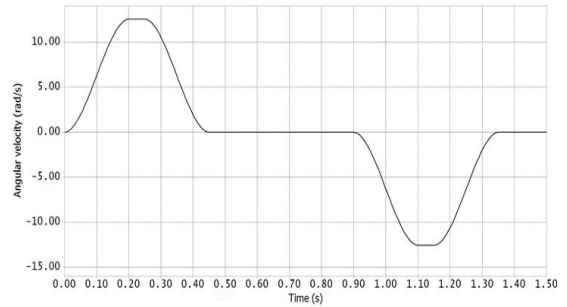
Axis 3



Axis 4



Axis 5



Axis 6

Fig. 5 Reference velocity profile for 6-axis

Table 2 Summary of reference angular velocity for driving torque calculation

| Axis | Cycle time used in analysis (s) | Acceleration and deceleration of the time (s) | Constant speed duration (s) | Reference angular velocity of constant speed duration (rad/s) |
|------|---------------------------------|---|-----------------------------|---|
| 1    | 3.11                            | 0.2   | 2.71                        | 1.91  |
| 2    | 6.71                            |   | 5.91                        | 0.92  |
| 3    | 3.80                            |   | 3.00                        | 1.71  |
| 4    | 4.92                            |   | 4.12                        | 0.80  |
| 5    | 2.10                            |   | 1.30                        | 0.80  |
| 6    | 1.35                            |   | 0.55                        | 0.55  |

Fig. 6 shows the reference angular velocity of axis 1 and the drive torque pattern simulated by RecurDyn<sup>®</sup> in the servo motor of axis 1 for a half-cycle. The maximum drive torque of axis 1 occurred during the acceleration period, and its value was  $312.69 N \cdot m$ .

Fig. 7 shows the reference angular velocity of axis 2 and the drive torque pattern simulated by RecurDyn<sup>®</sup> in the servomotor of axis 2 for a full cycle. The maximum drive torque of axis 2 occurred during the acceleration period, and its value was  $601.72 N \cdot m$ .

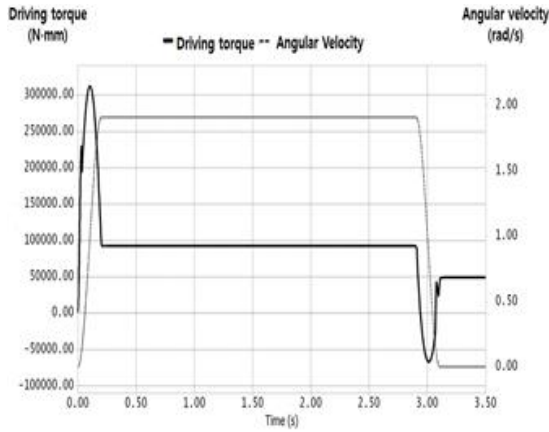


Fig. 6 Reference angular velocity profile and driving torque curve for Axis 1

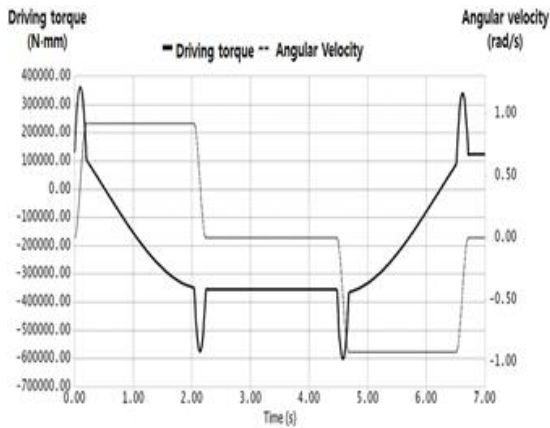


Fig. 7 Reference angular velocity profile and driving torque curve for Axis 2

The simulation results of all axes using the above method are summarized in Table 3. This evaluates the adequacy of the specifications of the motor and decelerator selected in the initial design stage by comparing the output torque considering the rated motor torque, reduction ratio, and reducer efficiency with the maximum drive torque. The evaluation results show that the specifications of the motor and reducer of every axis are adequate. The optimal design parameter values are listed in Table 4.

Table 3 Summary of simulation results

| Axis | Rated motor torque ( $N \cdot m$ ) | Output torque at rated speed ( $N \cdot m$ ) | Max. Driving torque ( $N \cdot m$ ) | Evaluation of appropriateness |
|------|------------------------------------|--|-------------------------------------|-------------------------------|
| 1    | 2.39                               | 313.51                                       | 312.69                              | OK                            |
| 2    | 4.78                               | 627.02                                       | 601.72                              | OK                            |
| 3    | 2.39                               | 285.80                                       | 252.91                              | OK                            |
| 4    | 0.48                               | 31.27  | 30.78                               | OK                            |
| 5    | 0.32                               | 22.29  | 11.54                               | OK                            |
| 6    | 0.32                               | 12.74  | 2.74                                | OK                            |

Table 4 Optimal design variables

| Design variables | Initial value | Optimal value |
|------------------|---------------|---------------|
| $D_1$ (mm)       | 54            | 53.28         |
| $D_2$ (mm)       | 54            | 55.79         |
| $W_1$ (mm)       | 77.59         | 77.32         |
| $W_2$ (mm)       | 155           | 155.16        |
| $W_3$ (mm)       | 215           | 216.13        |
| $l$ (mm)         | 170           | 172.47        |

## 4. Conclusions

This study investigated the optimization of the wrist shape of robots in the detailed design stage when the drive torque of the servo motor of a hollow six-axis robot did not meet the specifications of each joint's drive torque.

First, for application to the analysis of RecurDyn<sup>®</sup>, the dynamic analysis and calculation of the initial model were carried out considering the rotor inertia moment, reduction ratio, maximum rotation speed of the motor, and acceleration and deceleration time of the motor. As a result, for the end parts of the robot, the rated output torque of each axis did not reach the maximum drive torque. Therefore, the optimization design parameters of the robot were determined in the order of the upper arm, wrist, and

tool flange, which corresponded to the end parts of the robot.

Next, a simulation was performed in connection with RecurDyn® to optimize the design parameters  $D_1, D_2, W_1, W_2, W_3, l$  using the GA of MATLAB®. Consequently, the solution finally converged after 1,812 generations and the optimization was completed. It was found that the hollow size of the arm had to be increased to decrease the required drive torque for the end parts of the robot. Furthermore, the hollow servo motor and reducer were directly connected to the part  $D_1$ . Thus, it was considered that a smaller hollow size was ideal to reduce the cost of the hollow reducers, which increased exponentially with the hollow size.

In the optimal solution of the finally derived model, the rated output torque of each axis exceeded the maximum drive torque and satisfied the specifications of the motor and reducer. It was confirmed that GA can be used to optimize the wrist shape of the hollow six-axis articulated robot. In the future, we will research the robot risk optimization for various operation conditions.

## Acknowledgement

This research was supported by Changwon National University in 2017~2018.

## REFERENCES

1. Iqbal, J., "Automating Industrial Tasks Through Mechatronic Systems-A Review of Robotics In Industrial Perspective," *Hrčak.*, Vol. 23, No. 3, pp. 917-924, 2016.
2. Wang, Y. S., Ge, L. Z., Xie, P. C., Gai, Y. X., "Dynamic simulation and gravity balancing optimization of spot welding robot based on RecurDyn," *ICMA PROCEEDINGS.*, 2011.
3. Seibold, U., Kubler, B., Hirzinger, G., "Prototype of Instrument for Minimally Invasive Surgery with 6-Axis Force Sensing Capability," *ICMA PROCEEDINGS.*, pp.496-501, 2005.
4. Spong, M. W., "Robot Dynamics and Control," John Wiley and Sons Inc., 1989.
5. Jeon, Y. J., Lee, H. Y., Hong, D. S., "Selection of Major Components of a Four-Axis Transfer Robot through Dynamic Analysis," *ICMA PROCEEDINGS.*, p.590-595, 2017.
6. Hong, J. R., Jo, H. M., Chung, W. J., Park, S. K., Noh, S. H., "Implementation of a 2-axis Additional Axes Strategy on a 6-axis Articulated Robot for Improving Welding Process Efficiency," *Journal of the Korean Society of Manufacturing Process Engineers*, Vol. 16, No. 6, pp. 55-62, 2017.
7. Kang, S. J., Chung, W. J., Park, S. K., Noh, S. H., "A Study on Gain Scheduling Programming with the Fuzzy Logic Controller of a 6-axis Articulated Robot using LabVIEW®," *Journal of the Korean Society of Manufacturing Process Engineers.*, Vol. 16, No. 4, pp. 113-118, 2017.
8. RecurDyn® user manual and library manual, FunctionBay Inc., 2016.
9. Park, S. H., Chung, W. J., Kim, H. G., Choi, J. K., "Design and optimization of an efficient overboarding mechanism for the drop/lift automation of an active/passive sonar system in a surface ship," *ICMA PROCEEDINGS.*, 2015.